RSC Advances

ROYAL SOCIETY OF CHEMISTRY

www.rsc.org/advances

$Zr_xFe_{3-x}O_4$ ($0.01 \leq x \leq 1.0$) nanoparticles: a possible magnetic *in-vivo* switch

N. K. Prasad[a*], M. Srivastava[a], S. K. Alla[a], J. R. Danda[a,b] D. Aditya[a,c], and R. K. Mandal[a].

a. Department of Metallurgical Engineering, Indian Institute of Technology (Banaras Hindu University), Varanasi, 221005, India.

b. Mork Family Department of Chemical Engineering and Materials Science, University of Southern California, Los Angeles, CA, 90089-1211.

c. Department of Metallurgical Engineering and Material Science, Indian Institute of Technology, Bombay, Maharashtra - 400076

Abstract:

Magnetic hyperthermia holds promise for alternative therapeutic uses for cancer ailment having least side effects. It has issues pertaining to temperature rise during treatment. This work primarily discusses magnetic hyperthermia responses of nanoparticles of $Zr_xFe_{3-x}O_4$ ($0.01 \leq x \leq 1.0$) based ferrofluids of different concentrations. Structural characterization through x-ray diffraction (XRD) and selected area electron diffraction (SAD) patterns suggests formation of a single phase in the whole range of Zr-substituted Fe_3O_4. Even Energy Dispersive X-ray Spectrometry (EDX) analyses confirm doping of Zr^{4+} ions into Fe_3O_4. The observed variation in the saturation magnetizations (M_S) was found to be a function of concentration of Fe^{2+}, Fe^{3+} and Zr^{4+} ions at the interstitial voids of Fe_3O_4. The ferrofluids displayed stability near therapeutic temperature range (42-46 °C) for various combinations of amplitude and frequency of alternating magnetic field. The stability of temperature is unexpected in view of high Curie temperature (T_C > 300 °C). This behaviour of ferrofluid

was observed for a concentration up to 40 mg/mL of magnetic nanoparticles. Such an observation is lacking in literature available.

Keywords: Nanoparticles; Magnetic hyperthermia; specific absorption rate; *in-vivo* switch.

* *Corresponding author: nandkp.met@iitbhu.ac.in, Phone: 91-5422369346, Mobile: 91-9956629843, Fax: 91-5422369478.*

Introduction:

Extensive literature is available on the suitability of magnetic nanoparticles (MNPs) for various bioapplications [1-10]. Magnetic hyperthermia treatment of cancer is one of these applications. The desirable temperature range (42-46 °C) for this is achieved by a combined effect of hysteresis, Néel or Brwonian losses exhibited by magnetic nanoparticles (MNPs) in an alternating magnetic field. It holds promise for therapeutic uses to cure almost all kinds of tumors [1-9]. Generally, pure or substituted magnetite (Fe_3O_4) or maghemite (γ-Fe_2O_3) are used for the above purposes due to their suitable magnetic properties along with their large extent of biocompatibility [1-12]. Nevertheless, the continuous rise in the temperature during hyperthermia is inevitable with iron oxide based MNPs and chances of damage to the healthy tissues cannot be ruled out. The researchers have tried to monitor the temperature during hyperthermia using magneto resonance imaging (MRI) technique. However, it is found to be time consuming and expensive [13]. The other way to control this temperature rise is by using MNPs that have Curie temperature (T_C) in the therapeutic range (42-46 °C). As soon as the temperature reaches near T_C, they transform from ferromagnetic/ferrimagnetic to paramagnetic state and heating stops automatically. Such materials can act as an *in-vivo* switch. The materials based on such principle are $ZnGd_xFe_{2-x}O_4$, $Zn_xGd_{1-x}Fe$, $Ni_{1-x}Cr_x$, Cu–

Ni alloy and $La_{1-x}Sr_xMnO_3$ [14-16]. However, they suffer from two major drawbacks. They relate to low specific magnetization and inferior biocompatibility [14]. In a few research reports, it has been concluded that stable temperature below 50 °C can be achieved during hyperthermia with a lower concentration of MNPs (0.5 to 10 mg/mL) [17-19]. However, for clinical applications, one may need higher concentration of MNPs. Thus, getting a controlled heating with either pure or substituted ferrites (Fe_3O_4 or γ-Fe_2O_3) is a major challenge in magnetic hyperthermia or theranostic or drug delivery purposes.

In this work, we report an attainment of stable temperature (T_S) near 42 °C during hyperthermia for $Zr_xFe_{3-x}O_4$ ($0 \leq x \leq 1.0$) based ferrofluids. This effect was observed at different sets of amplitude and frequency of fields. It is important to note here that such a T_S has been observed for the samples with T_C values more than 300 °C. The details about $Zr_xFe_{3-x}O_4$ ($0.1 \leq x \leq 1.0$) nanoparticles are discussed in detail in our recent work [20].

Experimental

The synthesis protocols for $Zr_xFe_{3-x}O_4$ ($0.1 \leq x \leq 1.0$) nanoparticles can be found in reference [20]. Following such a protocol, we prepared $Zr_xFe_{3-x}O_4$ samples for $0 \leq x \leq 0.09$ to complete the series by same process [20]. For the sake of continuity, steps are given here in brief. The stoichiometric amounts of ferric chloride ($FeCl_3.7H_2O$), ferrous sulphate ($FeSO_4.xH_2O$) and zirconium oxychloride ($ZrOCl_2.8H_2O$) salts were dissolved in 200 mL of ethylene glycol (EG). NaOH pellets were added to get pH of the solution ~12. It was followed by microwave irradiation of solution. Precipitates obtained were washed and dried for further characterization. Oleic acid based ferrofluids of various concentrations of these MNPs were prepared.

The structural, microstructural and magnetic characterizations for $0.1 \leq x \leq 1.0$ samples are reported in earlier work [20]. For $0 \leq x \leq 0.09$ samples, the XRD patterns were

recorded with Cu K_α radiation (λ = 1.54056 Å) using an X-ray powder diffractometer (Rigaku Miniflex). Transmission electron microscope/high resolution TEM (FEI TechnaiG^2 20 S-Twin) was used to observe the morphology and size of the samples having x = 0.01, 0.06 and 1.0. For these samples, selected area electron diffraction (SAD) patterns were also recorded. To get information about approximate concentration of various elements at microscopic scale, the energy dispersive x-ray spectrometer (EDAX) attached to the scanning electron microscope (FEI Quanta 200F) was used. Magnetization *vs.* field up to ± 2 T and magnetization *vs.* temperature measurements at 0.2 T were carried out using SQUID (MPMS-XL, Quantum Design) to determine the M_S, M_r, H_C and T_C values. The heating rate of $Zr_xFe_{3-x}O_4$ ($0 \leq x \leq 1.0$) based ferrofluids at different sets of alternating current (ac) magnetic fields and frequencies were collected using MagneTherm (Nanotherics, UK) system. A copper-constantan thermocouple (T-type, Nanotherics, UK) was used as a sensor. The specific absorption rate (SAR) values were determined from temperature *vs.* time curves. It was calculated by the following formula [20].

$$\text{SAR (W/g MNP)} = \{(m_wC_w + m_mC_w)/m_m\}(dT/dt) \quad \text{W/g}$$

where, C_w = specific heat capacity water (4.186 $Jg^{-1}K^{-1}$), m_m and m_w are the mass of MNPs, and water respectively, dT/dt is the initial slope of the temperature vs. time curve.

Results and discussion:

The formation of single phase in the samples $Zr_xFe_{3-x}O_4$ ($0.1 \leq x \leq 1.0$) has been established by us [20]. For $0 \leq x \leq 0.09$, the samples $Zr_xFe_{3-x}O_4$ were also found to be monophasic based on XRD results (cf. figure 1). The Fe^{2+}, Fe^{3+} and Zr^{4+} ions were found to be distributed into both the tetrahedral and octahedral voids of Fe_3O_4 which has been confirmed from Reitveld analysis. Such a distribution of ions was due to the comparable ionic radii of the Fe and Zr ions. This was facilitated by possibility of ZrO_8 and ZrO_7 type coordination polyhedra in Zr-

O system. These are explained in reference [20]. The TEM/HRTEM micrographs of the samples with x = 0.01, 0.06 and 1.0 are given in the figures 2 (a), (b) and (c) respectively. The particles were in the range of 5-30 nm. The HRTEM image (figure 2 d) displays lattice spacing of ~ 0.29 nm corresponding to interplanar spacing of (220) plane spinel structure of Fe_3O_4. The SAD patterns of the samples conform to the spinel structure (cf. figures 2 (a), (b) and (c))

The SEM micrographs of as prepared $Zr_{0.1}Fe_{2.9}O_4$ and $ZrFe_2O_4$ samples are shown in Fig. 3 (a) and (c), respectively. The particles are nearly spherical in shape without discernible anisotropy and the estimated size was found to be ~50 nm. This is more than that estimated by TEM which is due to agglomeration of the particles. The EDX patterns were collected either from a single particle (shown encircled in the figures 3 (a) and (c)) or from the whole scanned area. The compositions of Zr, Fe, and O were same in both the cases and are given in the tables in figure 3. The Wt% (Obs) represents values obtained after EDX analysis whereas Wt% (Cal) indicates the value obtained from the chemical formula of $Zr_{0.1}Fe_{2.9}O_4$ and $ZrFe_2O_4$. This corroborates with the XRD and TEM findings of Zr-ion substitution on Fe-ions sites.

The variation of M_S, M_r and H_C obtained from Hysteresis loop for $Zr_xFe_{3-x}O_4$ ($0.01 \leq x \leq 1.0$) samples at room temperature and fields up to ± 2 T are shown in Fig. 4. The M_S values were lower than the value for bulk and pure Fe_3O_4 due to submicron sized particles in the present case. Figure 4 suggests that the M_S value is around 50 Am^2/kg for the samples up to x = 0.4. The variation in the M_S values for $x \leq 0.4$ samples can either be attributed to the distribution of Zr^{4+} ions at the two interstitial sites or to a small variation in the particles size. The significant decrease in the M_S value was observed for x = 0.6 and 1.0 samples. Explanation of such a decrease has been discussed in Ref. 20. It is presented here in brief.

From Reitveld analysis, it was established that the Fe^{3+} ions was equally distributed at both the sites for all samples. The amount of Zr^{4+} ions was relatively more at tetrahedral sites for $x \leq 0.4$ and at octahedral sites for $x > 0.4$ respectively. In contrast, Fe^{2+} ions were less at tetrahedral sites for $x \leq 0.4$ and octahedral sites for $x > 0.4$ respectively. Finally, the magnetization values were function of difference of Fe^{2+} ions at octahedral and tetrahedral sites. It has been observed that the variation in the calculated value of saturation magnetization for the samples was closely matching with the experimental values [20]. Due to lesser concentration of Fe^{2+} ions at tetrahedral sites, the M_S values were relatively more for samples with $0 \leq x \leq 0.09$. The low values of M_r and H_C are due to superparmagnetic nature of MNPs (Fig. 4 and in Ref. 20).

The magnetization *vs*. temperature curves at 50 mT for $Zr_xFe_{3-x}O_4$ ($0.01 \leq x \leq 1.0$) samples are given in Fig. 5. Their nature suggests that the $T_C > 300$ °C. It has been observed that the substitution of other ions like Mn, Zn, Al, Cu, Cr, Ti in Fe_3O_4 or γ-Fe_2O_3 are found to reduce the T_C value [21]. Out of these substitutions, the tetravalent Ti-ions found are more effective and could reduce T_C value to 100 °C [22].

The ferrofluids based on $Zr_xFe_{3-x}O_4$ ($0.01 \leq x \leq 1.0$) nanoparticles with a concentration of 40 mg/mL were subjected to an ac field of amplitude 25 mT and frequency 112 kHz. The temperature *vs*. time curves for all the ferrfluids are shown in Fig. 6. It is seen from this that fluids prepared using the samples of $x = 0.02$, 0.04, 0.05, 0.06 and 0.07 show T_S near 43, 47, 55, 37 and 38 °C respectively. Nevertheless, the other ferrofluids prepared using MNPs having $x = 0$ (i.e. Fe_3O_4) and $0.1 \leq x \leq 1.0$, display a continuous rise in temperature (> 60 °C) [20].

To investigate this aspect further, we carried out such experiments at different combinations of fields and frequencies. For example, in one combination of a field of

amplitude 23 mT and frequency of 173 kHz, the samples with x = 0.6, 0.8 and 0.9 displayed a continuous rise in temperature (Fig. 7). In contrast, the samples with x = 0.04, 0.06, 0.1 0.5 and 1.0 showed the T_S value 29, 33, 31, 39 and 40 °C respectively for these amplitude and frequencies (Fig. 7). It can be noted that the M_S value for the former samples were relatively smaller than these cf. Fig. 4. Thus, we found for some of the samples there was a continuous rise in temperature at one set of field and frequency while they displayed stability of temperature for another set (Fig. 7). The temperatures achieved during magnetic hyperthermia by different ferrofluids ($Zr_xFe_{3-x}O_4$, $0.01 \leq x \leq 1.0$) at different sets of field and frequencies are shown in figure 7. To indicate continuous rise in temperature during magnetic hyperthermia for various samples at different sets of field and frequency, the observed temperature was taken at or above 60 °C (Fig. 7). The same ferrofluid exhibited different T_S value at different sets of fields and frequencies. The heating ability of MNPs is dependent on field and frequency. In contrast, there was a continuous rise in the temperature during hyperthermia for Fe_3O_4, γ-Fe_2O_3 and Al-substituted γ-Fe_2O_3 at all sets of field and frequency (figure not given). We believe that such a phenomenon could be due to the presence of Zr^{4+} ions in the samples.

For more insight into this, we carried out hyperthermia experiment with the fluids of samples x = 0.01 and 0.5 at a field of an amplitude 23 mT and at a frequency 173 kHz having different concentration of MNPs (e.g. 5, 10, 20 and 40 mg/mL) as shown in Fig. 8 (a) and (b) respectively. The T_S value at 40 mg/mL concentration for x = 0.01 and 0.5 samples was 56 and 39 °C respectively (figure 8). For x = 0.01 based fluids, the T_S value rose to 40, 43 and 58 °C for the concentration 5, 10 and 20 mg/mL of MNPs respectively. The observations suggest that as the concentration of MNPs increases, the T_S value reached during hyperthermia also increases. Such behaviour is also found by other researchers [23]. The heating rate as well as T_S value for the fluid with a concentration 20 mg/mL was more than

that of 40 mg/mL for x = 0.01 sample (Fig. 8 a). This could be attributed to the dipolar interactions among the MNPs by which the overall magnetization reduces at higher concentration [24-26]. However, such interaction has negligible role on the T_S value with a concentration of 20 and 40 mg/mL. The fluid having MNPs with x = 0.5 also showed increase in the T_S value with higher concentration of MNPs (Fig. 8 b).

The stability of temperature during hyperthermia depending on amplitude and frequency of the magnetic field has not been reported in ferrofluids based on either pure or substituted Fe_3O_4 or γ-Fe_2O_3. Thus, we believe that new emergent magnetic phenomena appear in the presence of tetravalent Zr^{4+} ions in Fe_3O_4 owing to strong interaction amongst cations. Such a behavior seems lacking for other bivalent or trivalent substituted Fe_3O_4 or γ-Fe_2O_3. Possibly, Zr^{4+} ions might be influencing Fe^{2+} and Fe^{3+} ions in such a way that for a particular set of amplitude and frequency of the field and resultant magnetization starts decreasing in a manner to avoid further rise in temperature leading to T_S. This was even observed for the samples with x = 0.01, which suggests that even a minor addition of Zr-ions (Figs. 6, 7 and 8) is sufficient to display such a behaviour. The exact mechanism of stability of temperature during magnetic hyperthermia remains unclear to us. But, it is an important finding pertaining to a material that can serve as an *in-vivo* switch for magnetic hyperthermia, theranostic, drug delivery and MRI. The samples reported here has Zr^{4+} ions (well known biocompatible material) and thus will posses better biocompatibility than that of ferrites based systems reported earlier [8].

The SAR values of various samples at different set of field and frequencies are shown in Fig. 9. The figure indicates that the SAR values were not showing any particular variation with concentration. This could be attributed to the influence of Zr^{4+} ions on the magnetic properties and hence showed an unprecedented SAR values. In addition, the influence of amplitude and frequencies seems to be useful parameters for the desired SAR values. The

SAR values for different concentration of $Zr_{0.5}Fe_{2.5}O_4$ were not estimated as they displayed maximum T_S value below 39 °C. Contrary to this, the SAR value was 16.5, 15.9, 6.21 and 2.66 W/g at concentrations of 10, 20 and 40 mg/mL for $Zr_{0.01}Fe_{2.99}O_4$ MNPs. Higher SAR values at lower concentration of MNPs could be attributed to the comparatively slow decrease in the heating rate compared to the higher concentration. The SAR values are less than that some of the earlier reports but is comparable with other results [1, 7, 18, 20]. However, the SAR values are in the range for qualifying MNPs for their successful usage in magnetic hyperthermia.

Conclusions

This study reports successful preparation of single phase magnetic naoparticles of $Zr_xFe_{3-x}O_4$ for $0.01 \leq x \leq 1.0$. The substitution for whole range was confirmed from XRD, TEM and EDX analyses. The distribution of Fe^{2+}, Fe^{3+} and Zr^{4+} ions at the interstitial voids of Fe_3O_4 was the reason for the variation in M_S values. The ferrofluids of single phase $Zr_xFe_{3-x}O_4$ ($0.01 \leq x \leq 1.0$) system displayed a new phenomenon where stabilization of temperature (42-46 °C) could be achieved during hyperthermia by selecting a suitable set of frequency and amplitude of fields. Such a behaviour is unexpected as the synthesized materials have T_C higher than ambient temperature. It is believed that such a class of materials will open a new area of research for their potential uses in controlled hyperthermia, theranostic and drug delivery without causing significant damage to the healthy tissues.

Acknowledgement

The authors acknowledge DST, India for financial support to this work.

References

1. Jordan, A., R. Scholz, R.,Wust, P.,Schirra, H., Schiestel, T., Faehling, H.,Felix, R., *J. Magn. Magn. Mater,* **194**, 185-196(1999).

2. H.Lu, A. H., Salabas, E. L., Schüth, F., Angew. Chem., Angew.,*Int.Ed. Engl*., **46,** 1222-1244(2007).
3. Hafeli, U., Andra, W., Nowak, H., *Wiley-VCH, Weinheim*, **9**, 3745–3754(1998),.
4. Prasad, N.K., Bahadur, D., Vasseur, S., Duguet, E., *UK: John Wiley & Sons, Ltd,* 15-30(2008).
5. Thanh, N. T. K.,*Magnetic Nanoparticles: From Fabrication to Clinical Applications CRC Press*, (2012).
6. Shinde, S.S., Meena, S.S., Yusuf, S. M., Rajpure, K.Y., *J. Phys. Chem. C*, **115,** 3731-*3736*(2011).
7. Prasad, N. K., Rathinasamy, K., Panda, Bahadur, D., *J. Mater. Chem*., **17**, 5042-*5051*(2007). Prasad N. K. et al. Nanoparticles turn up the heat, Research highlight in *Nature Asia-Pacific, NPG Asia Materials*, Online 14th March, 2008, http://www.natureasia.com/asia-materials/highlight.php?id=72
8. Colombo, M., Romero, S. C., Casula, M. F., Gutie´rrez, L., Morales, M. P., Böhm, I. B., Heverhagen, T., Prosperi, D., Parak, W. J., *Chem. Soc. Rev*., **41**, 4306–4334(2012).
9. Thorat, N. D., Khot, V. M., Salunkhe, A. B., Ningthoujam, R. S., Pawar, S. H., *J. Colloids Surf. B: Bio interfaces,* **104,** 40-47(2013).
10. Gobbo, O. L., Sjaastad, K., Radomski, M. W., Volkov, Y., *A.Prina-Mello, Theranostics,* **5,**1249-1263(2015)
11. Prasad, N. K., Gohri, V., Bahadur, D., *J. Nanosc. Nanotech*.,2011, **11,** 2704-2710 (2011)
12. Fortin, J. P., Wilhelm, C., Servais, J., Menager, C., Bacri, J. C., Gazeau, F., *J. Am. Chem. Soc.*, **129**, 2628–2635(2007).
13. Maier-Hauff, K., Rothe, R., Scholz, R.., Gneveckow, U., Wust, P., Thiesen, B., Feussner, A., von Deimling, A., Waldoefner, N., Felix, R.., Jordan, A., *J. Neurooncol.*, **81**, 53(2007).
14. Prasad, N. K., Rathinasamy, K., Panda, Bahadur, D., *J. Biomed. Mater. Res. PartB : Appl. Biomater.*, **85B** , 409–416(2008).
15. Kuznetsov, A. A., Leontiev, V. G., Brukvin, V. A., Vorozhtsov, G. N., Ya. Kogan, B., Shlyakhtin, O. A., Yunin, A. M., Tsybin, O. I., Kuznetsov, O. A., *J. Magn. Magn. Mater,* **311**, 197-203(2007).
16. Vasseur, S., Duguet,E., Portie, J., Goglio, G., Mornet, S., Hadová, E., Knížek, K., Maryško, M., Veverka, P., Pollert, E., *J. Magn. Magn. Mater*, **302**, 315-320(2006).

17. Sadat, M. E., Patel, R.., Sookoor, J., Bud'ko, S. L., Ewing, R. C., Zhang, J., Xu, H., Wang, Y., Pauletti, G. M., Mast, D. B., Shi, D., *Mater. Sc. Engg. C*, **42**, 52–63(2014).
18. Mohapatra, J., Nigam, S., Gupta, J., Mitra, A., Aslam, M., Bahadur, D., *RSC Adv.*, **5**, 14311–14321 (2015).
19. Jeun, M., Bae, S., Tomitaka, A., Takemura, Y., Park, K. H., Paek, S. H., Chung, K. W., *Appl. Phys. Lett.* ,**95**, 082501(2009)
20. Gangwar, A., Alla, S. K., Srivastava, M., Meena, S. S., Prasadrao, E. V., Mandal, R. K., Yusuf, S. M., Prasad, N. K., (2016) *J. Magn. Magn. Mater,* **401**, 559–566.
21. Kinnari,P., Upadhyay, R.V., Mehta, R.V., *J. Magn. Magn.Mater*., **252**, 35–38(2002).
22. Butler, R. F., *Oxford: Blackwell Scientific, Boston*, (1992).
23. Mohapatra, J., Nigam, S. J., Gupta, J., Mitra, A., Aslam, M.., Bahadur, D., *RSC Adv.*, 2015, **5**, 14311–14321(2015).
24. Jeun, M., Bae, S., Tomitaka, A., Takemura, Y., Park, K. H., Paek, S. H., Chung, K. W., *Appl. Phys. Lett*.,**95**, 082501 (2009).
25. Urtizberea, A., Natividad, E., Arizaga, A., Castro, M., Mediano, A., *J. Phys. Chem. C*, **114**, 4916–4922 (2010).
26. Landi, G. T.,*Phys. Rev. B* ,**89**, 014403 (2014).

Figure caption

Figure 1: XRD patterns of $Zr_xFe_{3-x}O_4$ samples (a) x = 0.01, (b) x = 0.02, (c) x = 0.04, (d) x = 0.06 and e) x = 0.09.

Figure 2: TEM micrographs of a) $Zr_{0.01}Fe_{2.99}O_4$, b) $Zr_{0.06}Fe_{2.94}O_4$ and c) $ZrFe_2O_4$ samples. Insets show SAD patterns of the corresponding samples. d) The HRTEM micrograph of $ZrFe_2O_4$ sample.

Figure 3: a) SEM micrograph of $Zr_{0.1}Fe_{2.9}O_4$ sample, b) EDX pattern for $Zr_{0.1}Fe_{2.9}O_4$ sample, c) SEM micrograph of $ZrFe_2O_4$ sample and d) EDX pattern for $ZrFe_2O_4$ sample. Tables indicate concentration of Fe, Zr and O in $Zr_{0.1}Fe_{2.9}O_4$ and $ZrFe_2O_4$ samples in terms of Wt.% (Obs) and at. % as given by EDAX. The Wt% (Cal) refers the percentage concentration based on chemical formula of expected nominal composition.

Figure 4: The variation of M_S, M_r and H_C obtained from Hysteresis loop for $Zr_xFe_{3-x}O_4$ ($0.01 \leq x \leq 1.0$) samples at room temperature and fields up to ± 2 T.

Figure 5: The magnetization *vs*. temperature curves at 50 mT for $Zr_xFe_{3-x}O_4$ ($0.01 \leq x \leq 1.0$) samples.

Figure 6: The temperature *vs*. time curves for all the ferrfluids based on $Zr_xFe_{3-x}O_4$ ($0.01 \leq x \leq 1.0$) nanoparticles in an ac field of amplitude 25 mT and frequency 112 kHz.

Figure 7: The temperatures achieved during magnetic hyperthermia by different ferrofluids ($Zr_xFe_{3-x}O_4$, $0.01 \leq x \leq 1.0$) *vs*. Zr-concentration at different sets of field and frequencies.

Figure 8: Temperature vs. time curve at a field of an amplitude 23 mT and at a frequency 173 kHz having different concentration of MNPs (e.g. 5, 10, 20 and 40 mg/mL) for samples a) x = 0.01 and b) x = 0.5.

Figure 9: The SAR values of $Zr_xFe_{3-x}O_4$ ($0.01 \leq x \leq 1.0$) samples at different set of field and frequencies.

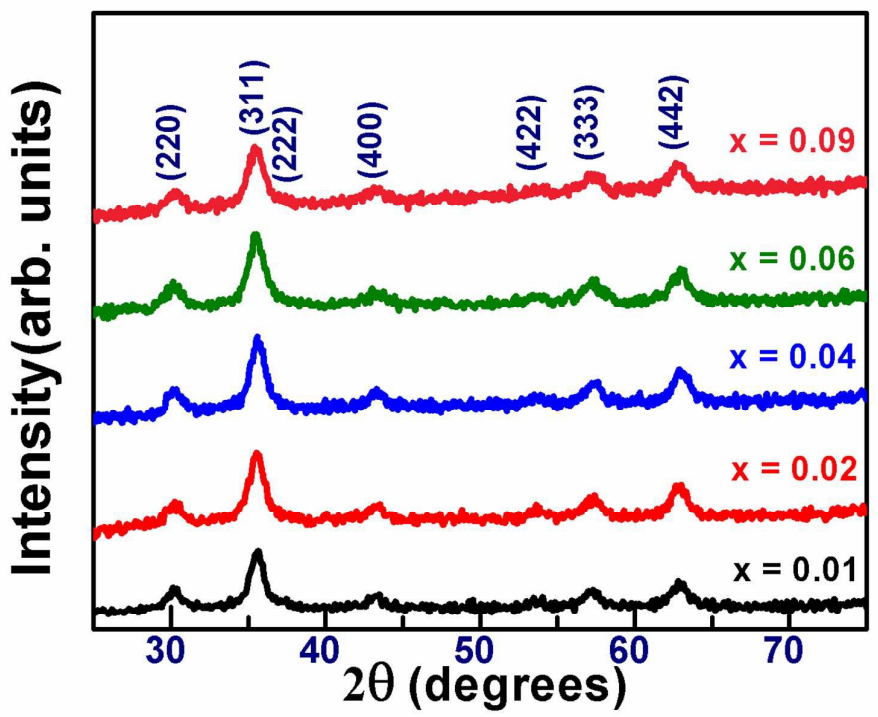

Figure 1

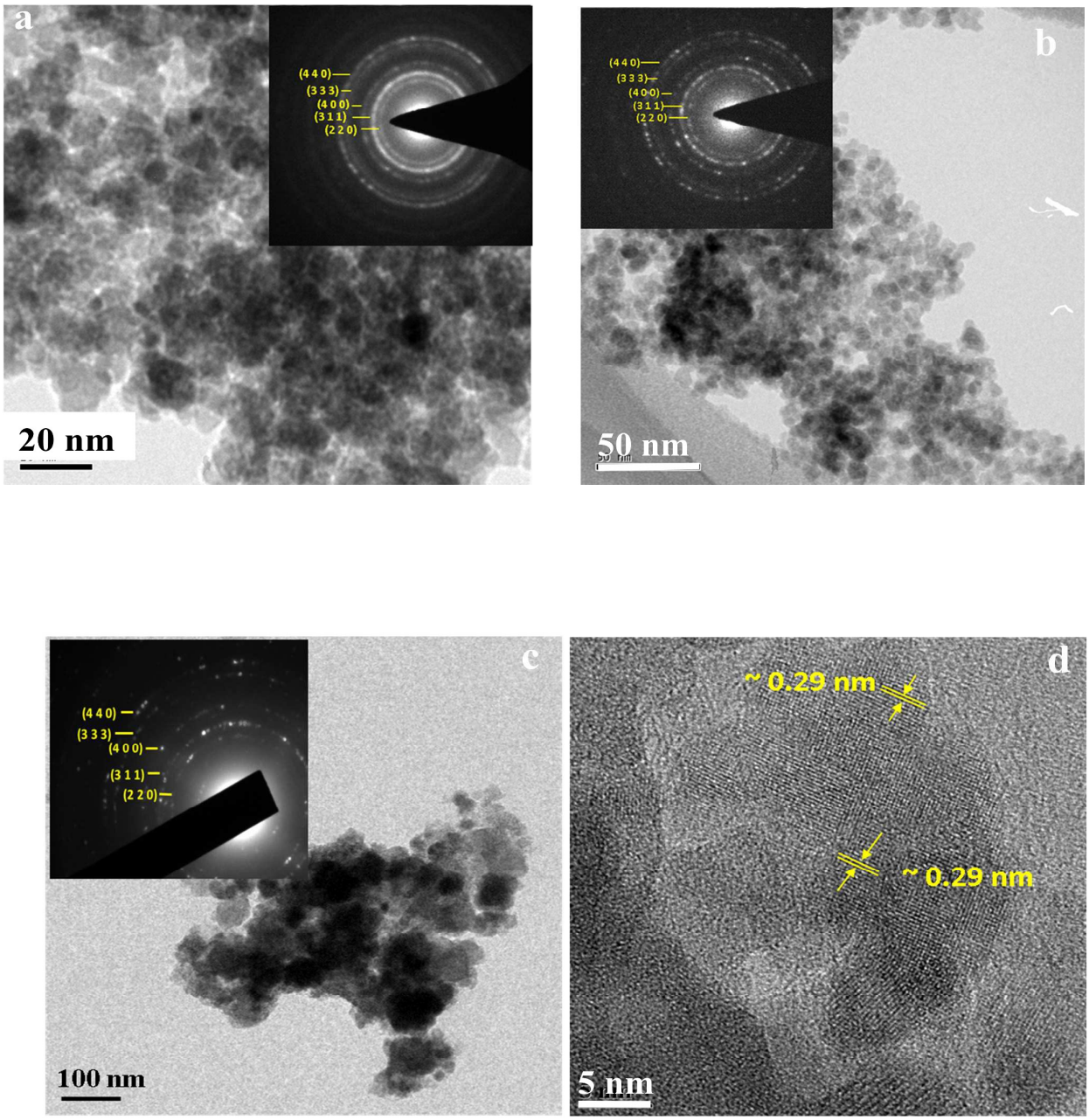

Figure 2

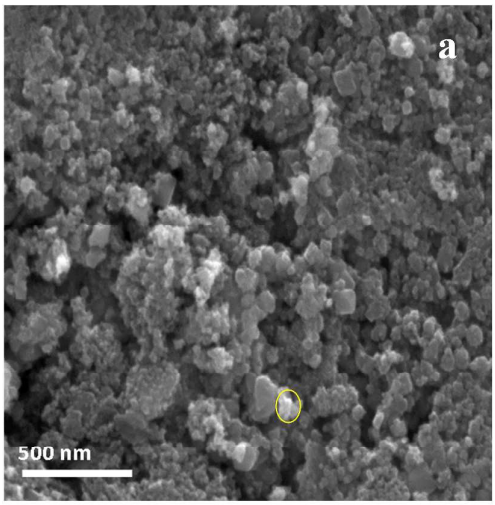

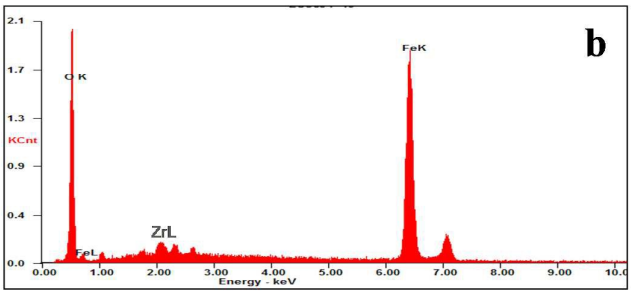

Element	Wt. % (Obs)	at%	Wt.% (Cal)
OK	27	58	25
ZrL	6	6	5
FeK	67	36	70

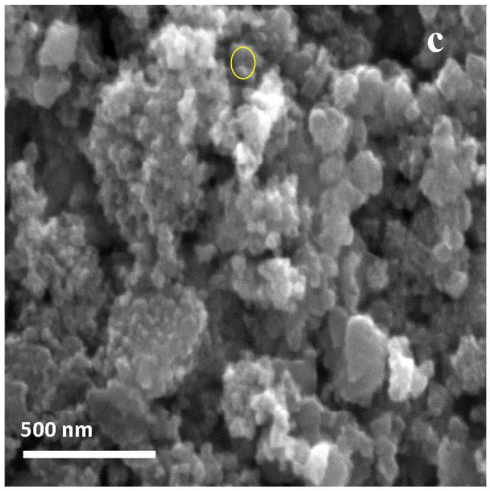

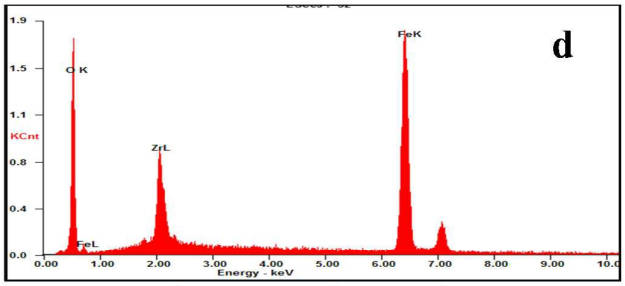

Element	Wt. % (Obs)	at%	Wt.% (Cal)
OK	24	58	23
ZrL	46	28	43
FeK	30	14	34

Figure 3

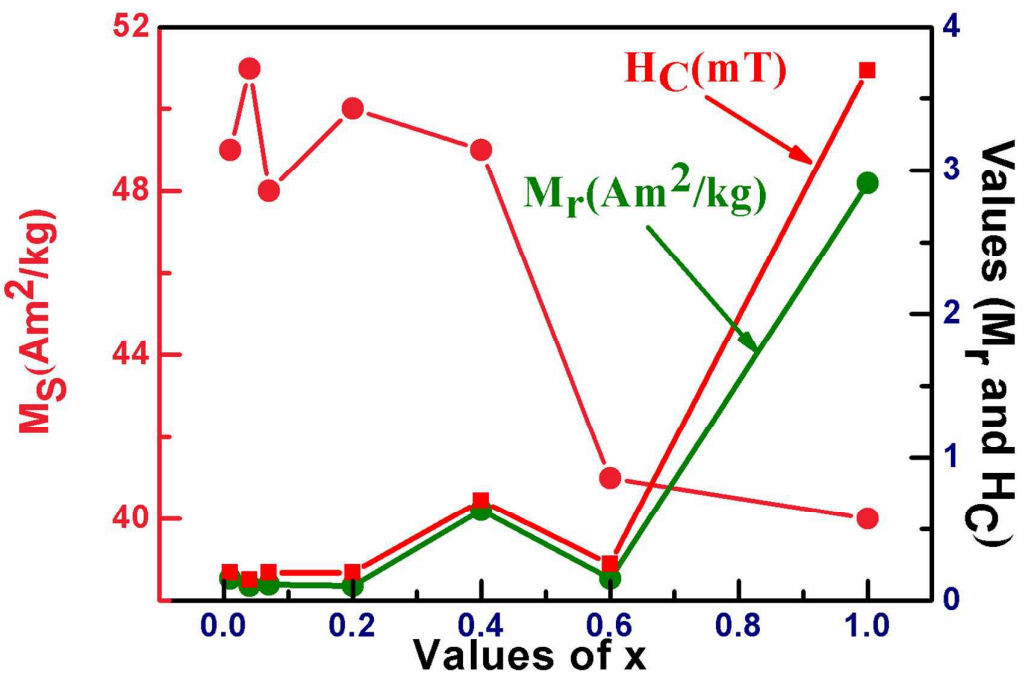

Figure 4

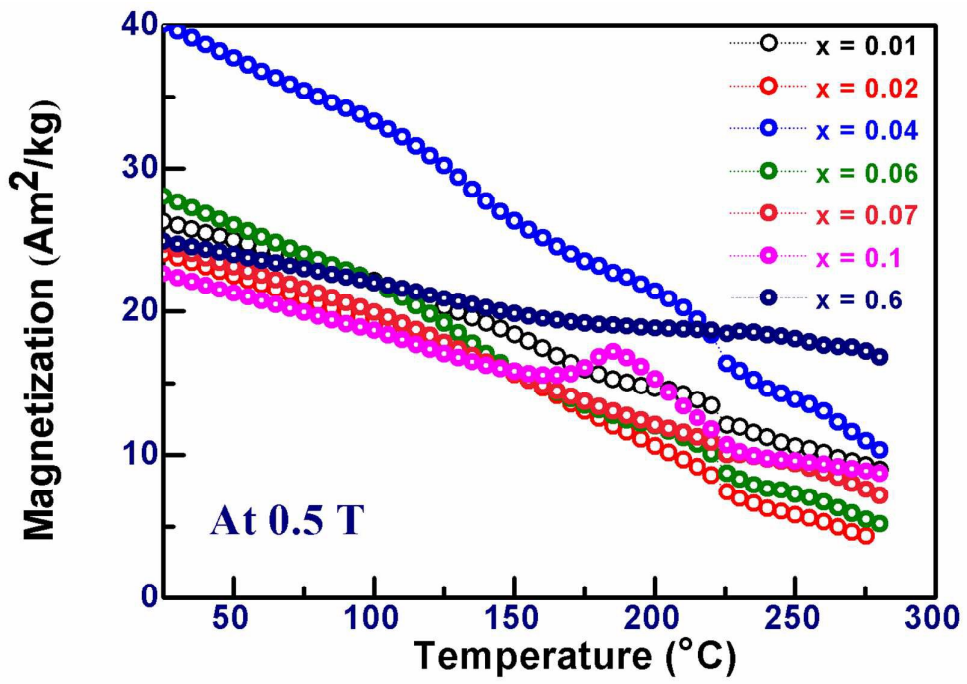

Figure 5

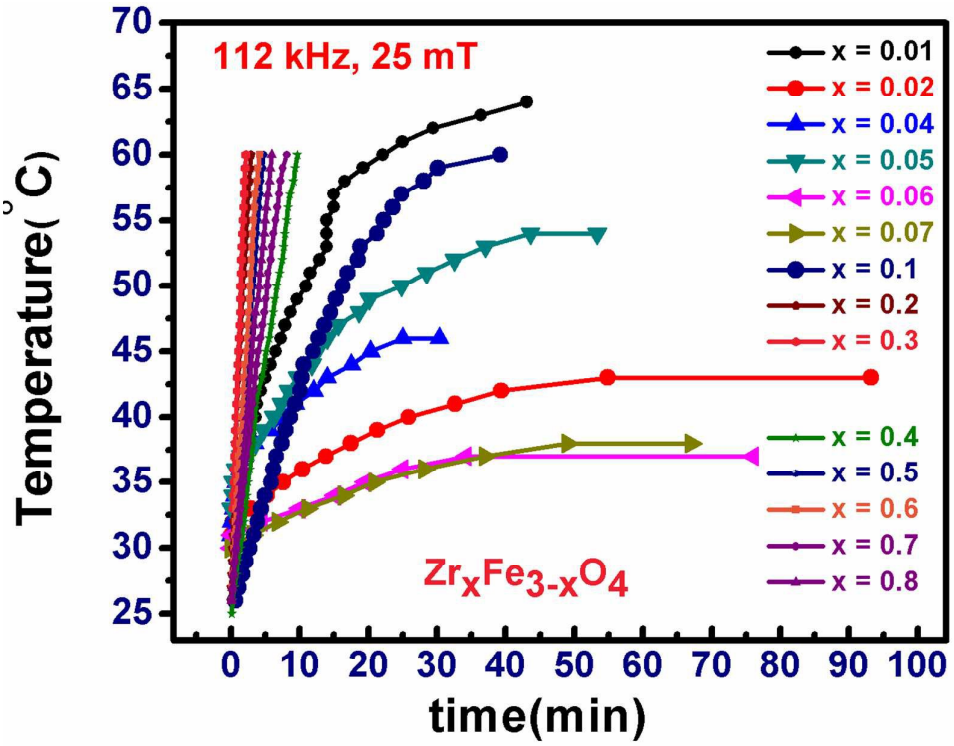

Figure 6

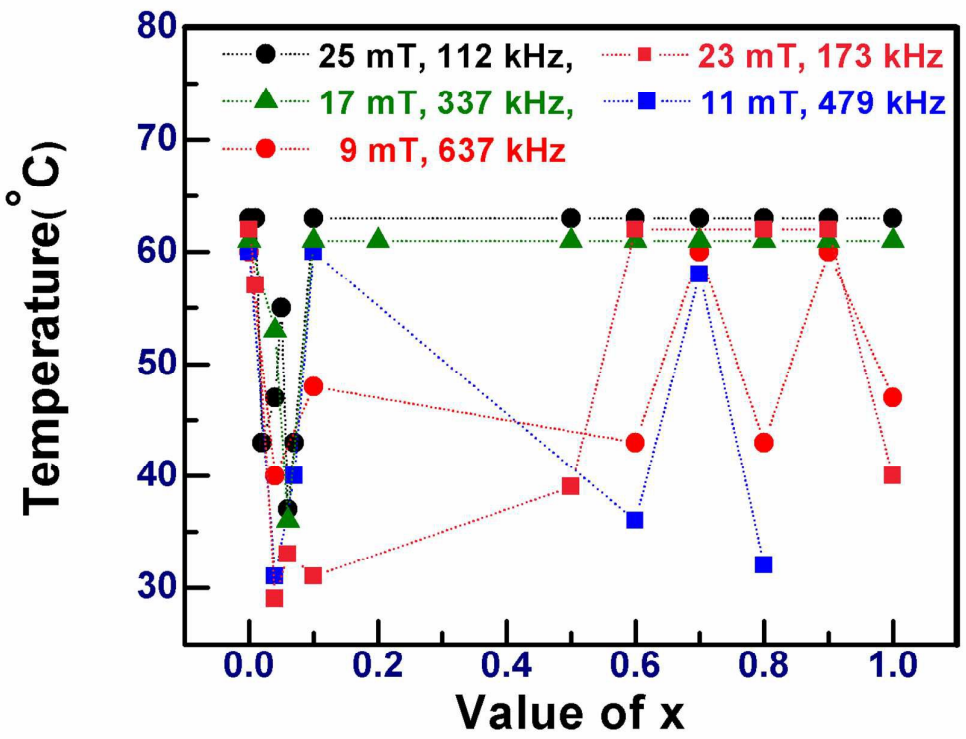

Figure 7

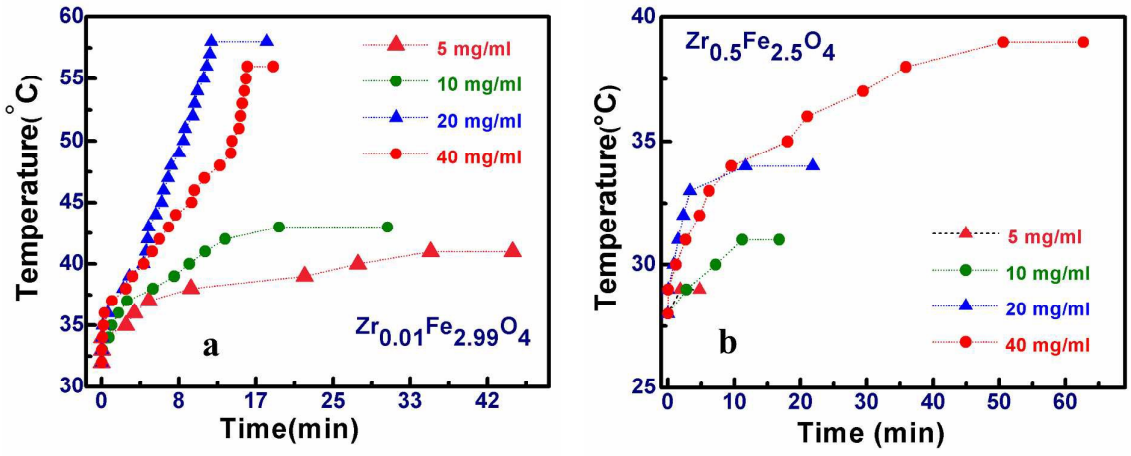

Figure 8

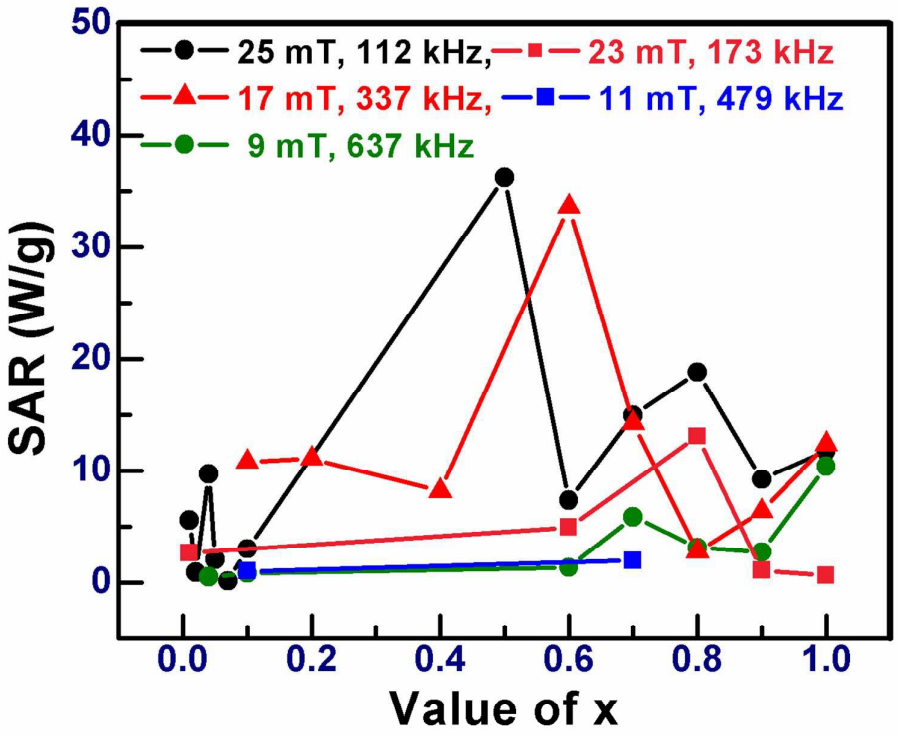

Figure 9